Energy Stability and Mixing Efficiency in Forced Stratified Shear Flows

Tobias Bischoff
supervised by Pascale Garaud and Basile Gallet

April 16, 2014

1 Introduction

Stratified flows are ubiquitous in nature. They occur in oceans, atmospheres and in the interiors of planets and stars. The density stratification in these systems can be caused by thermal gradients, i.e., the system is warm on one side and cold on the other, or by compositional gradients, such as induced by salt in the ocean (or other materials that impact the density of a fluid parcel). Stably stratified fluids are fluids in which the density gradient acts to stabilize the system against mixing. It is then often of interest to understand when mixing and transport can occur in the direction of the density gradient and how much transport can theoretically occur depending on the strength of the stratification. Turbulent properties such as the total heat and compositional fluxes, the total dissipation in the system, can be investigated using bounding techniques and direct numerical simulations.

In this report, we investigate simple stratified shear flows that are driven by an external body-force. Unlike flows that are driven on the boundaries, the forcing applies everywhere in the fluid. We investigate their energy stability properties and show that energy stability can be achieved in the case of strong stratifications for certain classes of stratified flows. We show how, at least in two dimensions, bounds for the viscous dissipation of the system can be extended from the unstratified case to the stratified case for any strength of the stratification. We then show that there exists a parameter regime in which the transport efficiency, i.e., the ratio of energy dissipation by vertical transport of heat to the total energy input per time, approaches one. This is confirmed by 2D direct numerical simulations.

We then further use direct numerical simulations to determine the dependence of the heat transport on the stratification. We find that there exist at least three regimes: For very strong stratification the laminar solution of the system is linearly stable and the heat transport is zero. In the regime of intermediate stratification, the system displays a bursting behavior, i.e., we observe mixing events followed by longer periods of episodic relaminarization of the flow. In the regime of weak stratifications the flow is fully chaotic. In two dimensions, we find that the flow field is dominated by large vortices at the forcing length scale, that advect the temperature field and dominate heat transport.

1.1 General Setup

The governing equations are the Boussinesq equations, in which density fluctuations are neglected except in the buoyancy force. In addition, we decompose the temperature field into a steady mean field with constant gradient T_{0z}, and a fluctuating field T so that the full set of equations reads

$$\frac{\partial \mathbf{u}}{\partial t} + \mathbf{u}\cdot\nabla\mathbf{u} = -\nabla p + \alpha g T \mathbf{e}_z + \nu\nabla^2\mathbf{u} + \mathcal{F}_0 f(kz)\mathbf{e}_x, \tag{1a}$$

$$\frac{\partial T}{\partial t} + \mathbf{u}\cdot\nabla T + wT_{0z} = \kappa_T\nabla^2 T, \tag{1b}$$

$$\nabla\cdot\mathbf{u} = 0, \tag{1c}$$

where

$$\frac{\rho}{\rho_0} = -\alpha T \tag{2}$$

defines the thermal expansion coefficient α. The other input parameters for this system are the gravitational constant g, the thermal diffusivity κ_T, the kinematic viscosity ν, the forcing amplitude $\mathcal{F}_0$ (with dimensions of an acceleration), and the forcing length scale k. Using the scales $[U] = (\mathcal{F}_0/k)^{1/2}$, $[t] = (k\mathcal{F}_0)^{-1/2}$, $[L] = k^{-1}$, and $[T] = T_{0z}/k$, we can nondimensionalize the governing equations (1a) to (1c). In addition, we assume that the perturbation equations are periodic in all directions so the nondimensional forcing profile $f(kz)$ must be a periodic function of the vertical coordinate. We also assume without loss of generality that $f(kz)$ is an odd function. After nondimensionalization, the governing equations become

$$\frac{\partial \mathbf{u}}{\partial t} + \mathbf{u}\cdot\nabla\mathbf{u} = -\nabla p + \mathrm{Ri} T\mathbf{e}_z + \frac{1}{\mathrm{Gr}_u^{1/2}}\nabla^2\mathbf{u} + f(z)\mathbf{e}_x, \tag{3a}$$

$$\frac{\partial T}{\partial t} + \mathbf{u}\cdot\nabla T + w = \frac{1}{\mathrm{Gr}_T^{1/2}}\nabla^2 T, \tag{3b}$$

$$\nabla\cdot\mathbf{u} = 0, \tag{3c}$$

where all quantitaties are nondimensional and where we introduced three nondimensional numbers that are based on the forcing amplitude $\mathcal{F}_0$. These nondimensional numbers are given by

$$\mathrm{Ri} = \frac{\alpha g T_{0z}}{k\mathcal{F}_0},\ \mathrm{Gr}_u^{1/2} = \frac{\mathcal{F}_0}{\nu^2 k^3} \text{ and } \mathrm{Gr}_T^{1/2} = \frac{\mathcal{F}_0}{\kappa_T^2 k^3} = \mathrm{Pr}^2\mathrm{Gr}_u^{1/2}, \tag{4}$$

where $\mathrm{Pr} = \nu/\kappa_T$ is the Prandtl number. The nondimensional number $\mathrm{Gr}_u^{1/2}$ is equivalent to a Reynolds number, but is based on the forcing amplitude and therefore usually called Grashof number. Equivalently, $\mathrm{Gr}_T^{1/2}$ corresponds to the Péclet number, but is based on the forcing amplitude.

The laminar solution of the system can be expressed in terms of the forcing function $f(z)$ and $\mathrm{Gr}_u^{1/2}$ with no background temperature fluctuations

$$\mathbf{u}_L = -\mathrm{Gr}_u^{1/2}\left(\partial_z^{-2} f(z)\right)\mathbf{e}_x, \tag{5a}$$

$$T_0 = 0. \tag{5b}$$

In the case of a Kolmogorov flow, the forcing profile $f(z)$ is given by $\sin(z)$ and the velocity field of the laminar solution is

$$\mathbf{u}_L = \mathrm{Gr}_u^{1/2} \sin(z)\mathbf{e}_x. \tag{6}$$

2 Energy stability of stratified shear flows

In this section we introduce the concept of energy stability to investigate some of the nonlinear stability properties of forced stratified shear flows. The first half of this section deals with the general case, where temperature perturbations can evolve freely. The second half of this section deals with the low Péclet number approximation and how it impacts energy stability. We find in the latter case that because the temperature perturbations are slaved to the perturbations in vertical velocity, we can derive a Richardson number criterion for energy stability, whereas we cannot derive such a result easily for the general case.

2.1 Energy stability theory

In this subsection, we investigate the energy stability of viscous stratified shear flows in two dimensions and apply it to the system introduced in the previous section. This is done by investigating the time evolution of an energy-like functional for perturbations to the laminar solution in Eq. (5a). We begin by letting $\mathbf{u} = \mathbf{u}_L + \tilde{\mathbf{u}}$, where $\tilde{\mathbf{u}} = (\tilde{u}, \tilde{w})$ is the perturbation velocity field. The governing equations then become

$$\frac{\partial \tilde{\mathbf{u}}}{\partial t} + \mathbf{u}_L \cdot \nabla \tilde{\mathbf{u}} + \tilde{\mathbf{u}} \cdot \nabla \mathbf{u}_L + \tilde{\mathbf{u}} \cdot \nabla \tilde{\mathbf{u}} = -\nabla p + \mathrm{Ri} T \mathbf{e}_z + \frac{1}{\mathrm{Gr}_u^{1/2}} \nabla^2 \tilde{\mathbf{u}} + f(z)\mathbf{e}_x, \tag{7a}$$

$$\frac{\partial T}{\partial t} + \mathbf{u}_L \cdot \nabla T + \tilde{\mathbf{u}} \cdot \nabla T + \tilde{w} = \frac{1}{\mathrm{Gr}_T^{1/2}} \nabla^2 T, \tag{7b}$$

$$\nabla \cdot \tilde{\mathbf{u}} = 0, \tag{7c}$$

and the "energy" equation for the perturbation velocity field $\tilde{\mathbf{u}}$ and the perturbation temperature field T takes the form

$$\frac{1}{2}\langle \tilde{\mathbf{u}}^2 + \gamma^2 T^2 \rangle_t = \left(\mathrm{Ri} - \gamma^2\right) \langle \tilde{w} T \rangle + \mathrm{Gr}_u^{1/2} \langle \tilde{u}\tilde{w}\partial_z^{-1} f \rangle - \frac{1}{\mathrm{Gr}_u^{1/2}} \langle |\nabla \tilde{\mathbf{u}}|^2 \rangle - \frac{\gamma^2}{\mathrm{Gr}_T^{1/2}} \langle |\nabla T|^2 \rangle, \tag{8a}$$

$$= (\Gamma - 1) \left(\frac{1}{\mathrm{Gr}_u^{1/2}} \langle |\nabla \tilde{\mathbf{u}}|^2 \rangle + \frac{\gamma^2}{\mathrm{Gr}_T^{1/2}} \langle |\nabla T|^2 \rangle \right), \tag{8b}$$

where

$$\Gamma = \frac{\left(\mathrm{Ri} - \gamma^2\right) \langle \tilde{w} T \rangle + \mathrm{Gr}_u^{1/2} \langle \left(\partial_z^{-1} f\right) \tilde{u}\tilde{w} \rangle}{\frac{1}{\mathrm{Gr}_u^{1/2}} \langle |\nabla \tilde{\mathbf{u}}|^2 \rangle + \frac{\gamma^2}{\mathrm{Gr}_T^{1/2}} \langle |\nabla T|^2 \rangle}. \tag{9}$$

Here, the inverse derivative in the vertical of the forcing function is given by $(\partial^{-1} f)(z) = -\mathrm{Gr}_u^{1/2} \partial_z u_L$ and is a measure of the shear applied to the flow. The angled brackets $\langle (.) \rangle$ denote the domain average (defined in the appendix). Since the second term in parentheses on the right hand side of (8b) is positive, this equation tells us that, for the energy to decay

in time, Γ needs to be less than 1. We are therefore interested in the maximum of Γ over all possible divergence-free flow fields, and over all possible temperature fields. This can be rexpressed as a maximization problem for the constrained Lagrangian

$$\mathcal{L} = \frac{\left(\mathrm{Ri} - \gamma^2\right)\langle \tilde{w}T\rangle + \mathrm{Gr}_u^{1/2}\langle\left(\partial_z^{-1} f\right)\tilde{u}\tilde{w}\rangle + \langle p\nabla\cdot\tilde{\mathbf{u}}\rangle}{\frac{1}{\mathrm{Gr}_u^{1/2}}\langle|\nabla\tilde{\mathbf{u}}|^2\rangle + \frac{\gamma^2}{\mathrm{Gr}_T^{1/2}}\langle|\nabla T|^2\rangle}, \tag{10}$$

where the divergence term in the numerator was introduced to satisfy the divergence-free constraint. The field p serves as the associated Lagrange multiplier. We need to find the maximum of the functional $\mathcal{L}$ with respect to the dynamical fields and the minimum with respect to the optimization constant γ^2. This can be done via the associated Euler-Lagrange equations derived from the first variation of $\mathcal{L}$. The Euler-Lagrange equations in two dimensions are given by the following four equations

$$\mathrm{Gr}_u^{1/2}\left(\partial_z^{-1} f\right)\tilde{w} - \partial_x p + \frac{2\Gamma}{\mathrm{Gr}_u^{1/2}}\nabla^2\tilde{u} = 0, \tag{11a}$$

$$\left(\mathrm{Ri} - \gamma^2\right)T + \mathrm{Gr}_u^{1/2}\left(\partial_z^{-1} f\right)\tilde{u} - \partial_z p + \frac{2\Gamma}{\mathrm{Gr}_u^{1/2}}\nabla^2\tilde{w} = 0, \tag{11b}$$

$$\left(\mathrm{Ri} - \gamma^2\right)\tilde{w} + \frac{2\Gamma\gamma^2}{\mathrm{Gr}_T^{1/2}}\nabla^2 T = 0, \tag{11c}$$

$$\nabla\cdot\tilde{\mathbf{u}} = 0, \tag{11d}$$

where the first one comes from the variation of $\mathcal{L}$ with respect to $\tilde{u}$, the second one comes from the variation of $\mathcal{L}$ with respect to $\tilde{w}$, the third one comes from the variation of $\mathcal{L}$ with respect to T and the last one comes from the variation of $\mathcal{L}$ with respect to p. Here, Γ is now treated as an eigenvalue of these PDEs. If $\Gamma < 1$ then $\min_{\gamma^2}\max_{\mathbf{u},T,p}\mathcal{L} < 1$ and the perturbations decay at least exponentially (apply Poincaré's inequality to equation (8b)). We now seek to solve the previous set of equations in order to determine the part of the parameter space for which the laminar solution is energy stable and the flow remains laminar for arbitrary perturbations. The equations can be simplified by taking the curl of the first two equations to remove the Lagrange multiplier. This leaves us with the following simplified set of equations

$$-\left(\mathrm{Ri} - \gamma^2\right)\partial_x T + \mathrm{Gr}_u^{1/2} f\tilde{w} - \mathrm{Gr}_u^{1/2}\left(\partial_z^{-1} f\right)\left(\partial_x\tilde{u} - \partial_z\tilde{w}\right) = -\frac{2\Gamma}{\mathrm{Gr}_u^{1/2}}\nabla^2\left(\partial_z\tilde{u} - \partial_x\tilde{w}\right), \tag{12a}$$

$$\left(\mathrm{Ri} - \gamma^2\right)\tilde{w} = -\frac{2\Gamma\gamma^2}{\mathrm{Gr}_T^{1/2}}\nabla^2 T, \tag{12b}$$

$$\nabla\cdot\tilde{\mathbf{u}} = 0, \tag{12c}$$

which can be simplified further by introducing the stream function ϕ for the components of the velocity field, i.e., $\tilde{u} = \partial_z\phi$ and $\tilde{w} = -\partial_x\phi$. This automatically satisfies the incompressibility constraint and allows us to rewrite the problem in terms of a system of linear

partial differential equations for two unknown fields only:

$$-\left(\mathrm{Ri}-\gamma^2\right)\partial_x T-\mathrm{Gr}_u^{1/2} f\partial_x\phi-2\mathrm{Gr}_u^{1/2}\left(\partial_z^{-1}f\right)\partial_{xz}\phi=-\frac{2\Gamma}{\mathrm{Gr}_u^{1/2}}\nabla^4\phi, \tag{13a}$$

$$-\frac{\left(\mathrm{Ri}-\gamma^2\right)}{\gamma^2}\partial_x\phi=-\frac{2\Gamma}{\mathrm{Gr}_T^{1/2}}\nabla^2 T. \tag{13b}$$

Finally, taking the Laplacian of the first equation and using the second one to replace the temperature field leaves a single partial differential equation for the stream function

$$-\frac{\mathrm{Gr}_T^{1/2}}{2\Gamma}\frac{\left(\mathrm{Ri}-\gamma^2\right)^2}{\gamma^2}\partial_{xx}\phi-\nabla^2(\mathrm{Gr}_u^{1/2} f\partial_x\phi+2\mathrm{Gr}_u^{1/2}\left(\partial_z^{-1}f\right)\partial_{xz}\phi)=-\frac{2\Gamma}{\mathrm{Gr}_u^{1/2}}\nabla^6\phi. \tag{14}$$

Expanding all fields in Fourier series (see appendix) in the x-direction results in a set of linear ordinary differential equations for the Fourier coefficients in the z-direction

$$\frac{\mathrm{Gr}_T^{1/2}}{2\Gamma}\frac{\left(\mathrm{Ri}-\gamma^2\right)^2}{\gamma^2}k_x^2\hat{\phi}-ik_x\left(\partial_{zz}-k_x^2\right)(\mathrm{Gr}_u^{1/2} f\hat{\phi}+2\mathrm{Gr}_u^{1/2}\left(\partial_z^{-1}f\right)\partial_z\hat{\phi})+\frac{2\Gamma}{\mathrm{Gr}_u^{1/2}}\left(\partial_{zz}-k_x^2\right)^3\hat{\phi}=0, \tag{15}$$

where $\hat{\phi}$ is the Fourier transform of the stream function and k_x is the horizontal wavenumber. This is a periodic boundary value problem in the vertical direction, which can either be solved using finite differences or by rewriting all z-dependent fields in terms of Fourier series as well, and then solving for the determinant of the resulting infinite dimensional matrix.

2.2 Example: Constant vertical shear

In this section, we investigate the energy stability of a flow field with constant vertical shear ($\partial_z u_L = S$). In this case, we do not need a forcing term as $\langle\nabla^2\mathbf{u}_L\rangle = 0$. We therefore set $f = 0$. While the total flow field $\mathbf{u}_L + \tilde{\mathbf{u}}$ is no longer periodic in z in this case, we can still assume that the perturbation field $\tilde{\mathbf{u}}$ is periodic. Also note that because there is no external forcing, we need to define the nondimensional parameters slightly differently. Given a constant shear profile $\mathbf{u}_L = Sz$, where S is the shear, we define the velocity scale $U = SL$, where L is the vertical extent of the domain. Length scales are normalized by L. The governing equations then look essentially the same as for the forced case with only the nondimensional numbers defined differently

$$\frac{\partial\mathbf{u}}{\partial t}+\mathbf{u}\cdot\nabla\mathbf{u}=-\nabla p+\mathrm{Ri}T\mathbf{e}_z+\frac{1}{\mathrm{Re}}\nabla^2\mathbf{u}, \tag{16a}$$

$$\frac{\partial T}{\partial t}+\mathbf{u}\cdot\nabla T+w=\frac{1}{\mathrm{Pe}}\nabla^2 T, \tag{16b}$$

$$\nabla\cdot\mathbf{u}=0. \tag{16c}$$

The nondimensional numbers based on the new length scale and velocity scale are given by

$$\mathrm{Ri}=\frac{\alpha g T_{0z}}{S^2},\ \mathrm{Re}=\frac{SL^2}{\nu}\text{ and }\mathrm{Pe}=\frac{SL^2}{\kappa_T}. \tag{17}$$

In this case, the analog of Eq. (15) (with Re, Pe instead of $\mathrm{Gr}_u^{1/2}$ and $\mathrm{Gr}_T^{1/2}$), with nondimensionalized laminar solution $u_L = z$, reduces to a set of algebraic equations in Fourier space (essentially setting $\mathrm{Gr}_u^{1/2}\left(\partial_z^{-1} f\right) = -1$ in Eq. (15)). Requiring nontrivial solutions allows us to determine the eigenvalues Γ. In this constant shear case there is no coupling of the Fourier modes and we have

$$\frac{\mathrm{Pe}}{2\Gamma\gamma^2}\left(\mathrm{Ri}-\gamma^2\right)^2 k_x^2\hat{\phi} + 2k_xk_z\left(k_x^2+k_z^2\right)\hat{\phi} - \frac{2\Gamma}{\mathrm{Re}}\left(k_x^2+k_z^2\right)^3\hat{\phi} = 0, \tag{18a}$$

$$\Rightarrow \left(\Gamma^2 - \mathrm{Re}\Gamma\frac{k_xk_z}{\left(k_x^2+k_z^2\right)^2} - \mathrm{PeRe}\frac{\left(\mathrm{Ri}-\gamma^2\right)^2}{4\gamma^2}\frac{k_x^2}{\left(k_x^2+k_z^2\right)^3}\right)\hat{\phi} = 0. \tag{18b}$$

The term in parentheses in Eq. (18b) needs to be 0. In order for this equation to have nontrivial solutions, the eigenvalues Γ need to satisfy

$$\Gamma = \frac{\mathrm{Re}k_xk_z}{2\left(k_x^2+k_z^2\right)^2} \pm \sqrt{\frac{\mathrm{Re}^2k_x^2k_z^2}{4\left(k_x^2+k_z^2\right)^4} + \mathrm{PeRe}\frac{\left(\mathrm{Ri}-\gamma^2\right)^2}{4\gamma^2}\frac{k_x^2}{\left(k_x^2+k_z^2\right)^3}}, \tag{19a}$$

$$= \frac{\mathrm{Re}k_xk_z}{2\left(k_x^2+k_z^2\right)^2}\left(1 \pm \sqrt{1+\frac{\mathrm{Pe}}{\mathrm{Re}}\frac{\left(\mathrm{Ri}-\gamma^2\right)^2}{\gamma^2}\frac{\left(k_x^2+k_z^2\right)}{k_z^2}}\right). \tag{19b}$$

The term involving the Richardson number under the square root is minimal for $\gamma^2 = \mathrm{Ri}$. Therefore, we have the case $\Gamma = 0$ and the case

$$\min_{\gamma^2}\Gamma = \frac{\mathrm{Re}k_xk_z}{\left(k_x^2+k_z^2\right)^2}. \tag{20}$$

Here, Γ is positive if k_x and k_z are either both positive or both negative. Without loss of generality, we assume positivity. Maximizing Γ with respect to k_x gives

$$\min_{\gamma^2}\max_{k_x}\Gamma = \mathrm{Re}\frac{3\sqrt{3}}{16}\frac{1}{k_z^2}, \tag{21}$$

for $k_x = k_z/\sqrt{3}$. The smallest (nondimensional) vertical wavenumber is given by 2π (see appendix Fourier transform) which maximizes Γ:

$$\min_{\gamma^2}\max_{k_z,k_x}\Gamma = \mathrm{Re}\frac{3\sqrt{3}}{64\pi^2}. \tag{22}$$

We require the maximum Γ to be less than 1 for energy stability. Hence, we arrive at a Reynolds number criterion for energy stability:

$$\mathrm{Re} < \frac{64\pi^2}{3\sqrt{3}}. \tag{23}$$

This implies that there is a critical Re above which the system will not be energy stable. Unfortunately, the critical Re is independent of the Richardson number, i.e, energy stability cannot be guaranteed for any Ri since there is always a value of Re above which the flow is not energy stable. In other words, even for very large Richardson numbers, the system is not energy stable and insight into the nonlinear evolution of arbitrary perturbations cannot be gained this way.

2.3 Example: Kolmogorov flow

In this section, we explore the first steps of the forced case for $f = \sin(z)$. The laminar solution is of Kolmogorov type and the governing equations are given by Eqs. (3). Taking Eq. (15) and expanding $\hat{\phi}$ in a Fourier series (see appendix) in the z-direction as

$$\hat{\phi}_{k_x}(z) = \sum_{k_z} \tilde{\phi}_{k_x,k_z} \exp(ik_z z). \tag{24}$$

This leaves us with terms of the form

$$f^{(q)}\hat{\phi}^{(p)}_{k_x} = i^p \sum_{k_z} {k_z}^p \tilde{\phi}_{k_x,k_z} f^{(q)} e^{ik_z z}, \tag{25}$$

where $f^{(q)}$ denotes the q-th derivative of f and $\hat{\phi}^{(p)}$ denotes the p-th derivative of $\hat{\phi}$. This determines the degree of mode coupling due to the presence of the shear forcing f. In the case of a Kolmogorov flow with $f = \sin(z)$, the derivatives $f^{(q)}$ are given by

$$f^{(q)} = \frac{1}{2} i^{q-1} \left(e^{iz} + (-1)^{q+1} e^{-iz} \right). \tag{26}$$

Taking the Fourier transform of the derivatives of the stream function ϕ into account, the quadratic coupling terms take the simple form

$$\left(f^{(q)}(z)\hat{\phi}^{(p)}_{k_x} \right)_{k_z} = \frac{1}{2} i^{p+q-1} \left((k_z - 1)^p \tilde{\phi}_{k_x,k_z-1} + (-1)^{q+1}(k_z + 1)^p \tilde{\phi}_{k_x,k_z+1} \right). \tag{27}$$

Here, the subscript k_z denotes the Fourier coefficient associated with the vertical wavenumber k_z. This relation allows us to rewrite Eq. (15) in terms of Fourier components, i.e., construct a simple matrix equation in wavenumber space

$$\frac{\Gamma}{\mathrm{Gr}_u^{1/2}} \tilde{\phi}_{k_x,k_z} = \Gamma^{-1} a(k_x,k_z)\tilde{\phi}_{k_x,k_z} + \mathrm{Gr}_u^{1/2} b(k_x,k_z)\tilde{\phi}_{k_x,k_z-1} + \mathrm{Gr}_u^{1/2} c(k_x,k_z)\tilde{\phi}_{k_x,k_z+1}. \tag{28}$$

Setting $\Gamma = 1$ implies that the critical Grashof number, at a given horizontal wavenumber k_x, at which instability occurs, is given by the solution of

$$a(k_x,k_z)\tilde{\phi}_{k_x,k_z} + \mathrm{Gr}_u^{1/2} b(k_x,k_z)\tilde{\phi}_{k_x,k_z-1} + \mathrm{Gr}_u^{1/2} c(k_x,k_z)\tilde{\phi}_{k_x,k_z+1} - \frac{1}{\mathrm{Gr}_u^{1/2}} \tilde{\phi}_{k_x,k_z} = 0. \tag{29}$$

The k_x and k_z-dependent coefficients define a matrix with

$$a(k_x,k_z) = \frac{\mathrm{Gr}_T^{1/2} \left(\mathrm{Ri} - \gamma^2 \right)^2 {k_x}^2}{4\gamma^2 \left({k_x}^2 + {k_z}^2 \right)}, \tag{30a}$$

$$b(k_x,k_z) = \frac{k_x {k_z}^2 (2k_z - 1) - {k_x}^3 (1 - 2k_z)}{2 \left({k_x}^2 + {k_z}^2 \right)^3}, \tag{30b}$$

$$c(k_x,k_z) = \frac{k_x {k_z}^2 (2k_z + 1) + {k_x}^3 (1 + 2k_z)}{2 \left({k_x}^2 + {k_z}^2 \right)^3}. \tag{30c}$$

We can find the critical Grashof number by determining for which $\mathrm{Gr}_u^{1/2}$ the determinant of this matrix is zero. Because the determinant defines a function of $\mathrm{Gr}_u^{1/2}$, this problem can be solved with a root-finding algorithm. However, these last steps will be subject of future work.

2.4 The low Péclet number approximation

In this section we derive the low thermal Grashof number equations from the forced Boussinesq equations (3). This is equivalent to what is usually called the "low Péclet number approximation", an approximation commonly made in the context of astrophysics [7, 8, 10]. It holds for very low Prandtl numbers. At the same time, we require the Richardson number to be large. In fact, we require it to be of order $1/\mathrm{Gr}_T^{1/2}$. In order to derive this approximation, we write the dynamical fields formally as asymptotic expansions in the $\mathrm{Gr}_T^{1/2}$

$$\mathbf{u} = \mathbf{u}_0 + \mathrm{Gr}_T^{1/2}\,\mathbf{u}_1 + \dots, \tag{31a}$$

$$T = T_0 + \mathrm{Gr}_T^{1/2}\,T_1 + \dots . \tag{31b}$$

The governing equations at order $\mathrm{Gr}_T^{1/2}$ reduce to Laplace's equation for the zeroth order temperature fluctuation

$$\nabla^2 T_0 = 0, \tag{32}$$

which, in the case of a periodic domain, requires $T_0 = 0$. At the next order, the governing equations read

$$\frac{\partial \mathbf{u}_0}{\partial t} + \mathbf{u}_0 \cdot \nabla \mathbf{u}_0 = -\nabla p_0 + \tilde{\mathrm{Ri}} T_1 \mathbf{e}_z + \frac{1}{\mathrm{Gr}_u^{1/2}} \nabla^2 \mathbf{u}_0 + f(z)\mathbf{e}_x, \tag{33a}$$

$$w_0 = \nabla^2 T_1, \tag{33b}$$

$$\nabla \cdot \mathbf{u}_0 = 0, \tag{33c}$$

where we replaced Ri by $\mathrm{Ri} = \tilde{\mathrm{Ri}}/\mathrm{Gr}_T^{1/2}$ and assumed $\tilde{\mathrm{Ri}} = \mathcal{O}(1)$. This can be combined to give a more compact set of integro-differential equations:

$$\frac{\partial \mathbf{u}_0}{\partial t} + \mathbf{u}_0 \cdot \nabla \mathbf{u}_0 = -\nabla p_0 + \tilde{\mathrm{Ri}} \nabla^{-2} w_0 \mathbf{e}_z + \frac{1}{\mathrm{Gr}_u^{1/2}} \nabla^2 \mathbf{u}_0 + f(z)\mathbf{e}_x, \tag{34a}$$

$$\nabla \cdot \mathbf{u}_0 = 0. \tag{34b}$$

From this perspective, we see that the important nondimensional parameter that controls the importance of the stratification is $\mathrm{RiGr}_T^{1/2} = \tilde{\mathrm{Ri}}$. We also see that T drops out entirely so that the energy stability can now be investigated simply by analyzing the time evolution of the kinetic energy in the perturbation field.

2.5 Energy Stability in the low Péclet number limit: Bounds

In this section, we derive a Richardson number criterion for the energy stability of the laminar solution of a forced stratified shear flow in the low Péclet/low thermal Grashof number limit. We proceed as before, but this time we begin with the kinetic energy equation for arbitrary perturbation to the laminar solution. With $\mathbf{u} = \mathbf{u}_L + \tilde{\mathbf{u}}$, we have

$$\frac{1}{2}\langle \tilde{\mathbf{u}}^2 \rangle_t = \mathcal{H}\left[\tilde{\mathbf{u}}\right] = \tilde{\mathrm{Ri}} \langle \tilde{w} \nabla^{-2} \tilde{w} \rangle + \mathrm{Gr}_u^{1/2} \langle \left(\partial_z^{-1} f\right) \tilde{w} \tilde{u} \rangle - \frac{1}{\mathrm{Gr}_u^{1/2}} \langle |\nabla \tilde{\mathbf{u}}|^2 \rangle. \tag{35}$$

Here, $\mathcal{H}[\tilde{\mathbf{u}}]$ is a quadratic form of the velocity perturbations only. The task at hand is to show that for all parameters of the system there exists a value of the Richardson number so that the quadratic form is negative semi-definite. Such a criterion defines the region of parameter space in which the system is energy stable. We approach the problem using simple bounding methods instead of the optimization technique used in the previous sections. We start with a conventional estimate for the triple term involving the shear term

$$|\langle\left(\partial_z^{-1} f\right)\tilde{w}\tilde{u}\rangle| \leq ||\partial_z^{-1} f||_\infty \langle\tilde{w}\tilde{u}\rangle \leq \frac{||\partial_z^{-1} f||_\infty}{2}\left(\frac{1}{a}\langle\tilde{w}^2\rangle + a\langle\tilde{u}^2\rangle\right). \tag{36}$$

Here, we used the Young's inequality $|ab| < 1/2(a^2+b^2)$ (see appendix). Of course, this gives a very crude estimate, because the right hand side is positive and we want to estimate a potentially negative term. The free parameter a introduced will give some freedom in the rest of the derivation. Using the estimate (36) to bound the quadratic form from above, we get

$$\mathcal{H}[\tilde{\mathbf{u}}] \leq -\tilde{\mathrm{Ri}}\langle(\nabla^{-1}\tilde{w})^2\rangle + \frac{\mathrm{Gr}_u^{1/2}}{2}||\partial_z^{-1} f||_\infty\left(\frac{1}{a}\langle\tilde{w}^2\rangle + a\langle\tilde{u}^2\rangle\right) - \frac{1}{\mathrm{Gr}_u^{1/2}}\langle|\nabla\tilde{\mathbf{u}}|^2\rangle, \tag{37a}$$

$$\leq \sum_{\mathbf{k}} \frac{\mathrm{Gr}_u^{1/2}}{2}||\partial_z^{-1} f||_\infty\left(\frac{1}{a}|\tilde{w}_{\mathbf{k}}|^2 + a|\tilde{u}_{\mathbf{k}}|^2\right) - \frac{\tilde{\mathrm{Ri}}}{\mathbf{k}^2}|\tilde{w}_{\mathbf{k}}|^2 - \frac{\mathbf{k}^2}{\mathrm{Gr}_u^{1/2}}\left(|\tilde{u}_{\mathbf{k}}|^2 + |\tilde{w}_{\mathbf{k}}|^2\right), \tag{37b}$$

$$\leq \sum_{\mathbf{k}}\left(\frac{\mathrm{Gr}_u^{1/2}}{2a}||\partial_z^{-1} f||_\infty - \frac{\tilde{\mathrm{Ri}}}{\mathbf{k}^2} - \frac{\mathbf{k}^2}{\mathrm{Gr}_u^{1/2}}\right)|\tilde{w}_{\mathbf{k}}|^2 + \left(a - \frac{1}{\mathrm{Gr}_u^{1/2} L_{\max}^2}\right)|\tilde{u}_{\mathbf{k}}|^2, \tag{37c}$$

where we used the periodicity of the system to write all fields in terms of their Fourier expansions (see appendix) and made use of the finite size of the system with largest length scale $L_{\max}$. In the second line, we also replaced the Fourier coefficients of the temperature field in terms of the Fourier coefficients of the vertical velocity. A sufficient criterion for energy stability can be obtained by requiring that the expressions in the parentheses are negative. The first parenthesis is of the form

$$F(X) = A - BX^{-2} - CX^2, \tag{38}$$

which has a maximum as

$$F_{\max} = A - 2\sqrt{BC}. \tag{39}$$

Therefore, we can estimate the quadratic form from above by using the maximum of F(X) for the worst-case-scenario:

$$\mathcal{H}[\tilde{\mathbf{u}}] \leq \sum_{\mathbf{k}}\left(\frac{\mathrm{Gr}_u^{1/2}}{2a}||\partial_z^{-1} f||_\infty - 2\left(\frac{\tilde{\mathrm{Ri}}}{\mathrm{Gr}_u^{1/2}}\right)^{\frac{1}{2}}\right)|\tilde{w}_{\mathbf{k}}|^2 + \left(a - \frac{1}{\mathrm{Gr}_u^{1/2} L_{\max}^2}\right)|\tilde{u}_{\mathbf{k}}|^2. \tag{40}$$

We want the $1/a$ term in the first parenthesis to be as small as possible provided that the second parenthesis remains negative. Hence, a suitable a is $a = 1/(2\mathrm{Gr}_u^{1/2} L_{\max}^2)$. Inserting this into the previous estimate, we arrive at

$$\mathcal{H}[\tilde{\mathbf{u}}] \leq \left(\mathrm{Gr}_u L_{\max}^2 ||\partial_z^{-1} f||_\infty - 2\left(\frac{\tilde{\mathrm{Ri}}}{\mathrm{Gr}_u^{1/2}}\right)^{\frac{1}{2}}\right)\langle\tilde{w}^2\rangle - \frac{1}{2\mathrm{Gr}_u^{1/2} L_{\max}^2}\langle\tilde{u}^2\rangle < 0. \tag{41}$$

We can then pick a Richardson number to let the expression in the first parenthesis remain negative for all other system parameters, i.e.,

$$\tilde{\mathrm{Ri}} > \frac{L_{\max}^4}{2} ||\partial_z^{-1} f||_\infty^2 \, \mathrm{Gr}_u^{5/2}. \tag{42}$$

We see that the Richardson number needs to be very large when $\mathrm{Gr}_u^{1/2}$ is large or when the size of the domain itself is very large. Interestingly, it depends on the shear only through the maximum value of $\partial_z^{-1} f$ and the "shape" of f does not enter. In contrast to the general case, we now have a stability criterion that does indeed depend on Ri through $\tilde{\mathrm{Ri}}$, i.e., the strength of the stratification. This is a direct consequence of the fact that the temperature field is completely determined by the vertical velocity, a key assumption of this approximation.

2.6 Energy Stability in the low Péclet number limit: Analysis

We now want to investigate the full energy stability similar to what was done in section 2.1. For that we start in the same fashion, i.e., by using the perturbation energy equation. From there, we can straightforwardly derive the Euler-Lagrange equations for the problem and understand the differences to the full problem. The kinetic energy equation in the low $\mathrm{Gr}_T^{1/2}$ limit is given by Eq. (35). From this, we can define a quadratic form $\mathcal{H}[\mathbf{u}]$ that can be written in a similar way as before

$$\mathcal{H}[\tilde{\mathbf{u}}] = -\tilde{\mathrm{Ri}}\langle|\nabla^{-1}\tilde{w}|^2\rangle + \mathrm{Gr}_u^{1/2}\langle\left(\partial_z^{-1} f\right)\tilde{w}\tilde{u}\rangle - \frac{1}{\mathrm{Gr}_u^{1/2}}\langle|\nabla\tilde{\mathbf{u}}|^2\rangle, \tag{43a}$$

$$= \frac{1}{\mathrm{Gr}_u^{1/2}}\langle|\nabla\tilde{\mathbf{u}}|^2\rangle \left(\frac{-\tilde{\mathrm{Ri}}\langle|\nabla^{-1}\tilde{w}|^2\rangle + \mathrm{Gr}_u^{1/2}\langle\left(\partial_z^{-1} f\right)\tilde{w}\tilde{u}\rangle}{\frac{1}{\mathrm{Gr}_u^{1/2}}\langle|\nabla\tilde{\mathbf{u}}|^2\rangle} - 1 \right), \tag{43b}$$

$$= \frac{1}{\mathrm{Gr}_u^{1/2}}\langle|\nabla\tilde{\mathbf{u}}|^2\rangle \left(\Gamma - 1\right), \tag{43c}$$

$$\tag{43d}$$

where

$$\Gamma = \frac{-\tilde{\mathrm{Ri}}\langle|\nabla^{-1}\tilde{w}|^2\rangle + \mathrm{Gr}_u^{1/2}\langle\left(\partial_z^{-1} f\right)\tilde{w}\tilde{u}\rangle}{\frac{1}{\mathrm{Gr}_u^{1/2}}\langle|\nabla\tilde{\mathbf{u}}|^2\rangle}. \tag{44}$$

We need to determine the maximum of Γ over all divergence-free vector fields $\tilde{\mathbf{u}}$ as before. This leads to an equivalent maximization problem for the Lagrangian

$$\mathcal{L} = \left(\frac{-\tilde{\mathrm{Ri}}\langle|\nabla^{-1}\tilde{w}|^2\rangle + \mathrm{Gr}_u^{1/2}\langle\left(\partial_z^{-1} f\right)\tilde{w}\tilde{u}\rangle + \langle p\nabla\cdot\tilde{\mathbf{u}}\rangle}{\frac{1}{\mathrm{Gr}_u^{1/2}}\langle|\nabla\tilde{\mathbf{u}}|^2\rangle} \right). \tag{45}$$

Analogously, the maximum has to solve the following Euler-Lagrange equations in two dimensions

$$\mathrm{Gr}_u^{1/2}\left(\partial_z^{-1} f\right)\tilde{w} + \frac{2\Gamma}{\mathrm{Gr}_u^{1/2}}\nabla^2\tilde{u} - \partial_x p = 0, \tag{46a}$$

$$2\tilde{\mathrm{Ri}}\nabla^{-2}\tilde{w} + \mathrm{Gr}_u^{1/2}\left(\partial_z^{-1} f\right)\tilde{u} + \frac{2\Gamma}{\mathrm{Gr}_u^{1/2}} - \partial_z p = 0. \tag{46b}$$

These are similar to the ones for the general case, but now include a nonlocal term in the second equation that helps to control the vertical component of the perturbation velocity field. Again, taking the curl and introducing a stream function ϕ yields the following integro-partial differential equation

$$2\tilde{\mathrm{Ri}}\partial_x\left(\nabla^{-2}\partial_x\phi\right) - \mathrm{Gr}_u^{1/2} f\partial_x\phi - 2\mathrm{Gr}_u^{1/2}\left(\partial_z^{-1} f\right)\partial_{xz}\phi = -\frac{2\Gamma}{\mathrm{Gr}_u^{1/2}}\nabla^4\phi. \tag{47}$$

As an example, although slightly artificial, we consider again the constant shear case, i.e., we investigate the energy stability of the solution $\mathbf{u}_L = Sz$ with respect to spatially periodic perturbations $\tilde{\mathbf{u}}$. Just like in Section 2.2, we consider the system to be unforced and the velocity scale to be SL, with L being the vertical domain size (i.e, we consider Re, Pe instead of $\mathrm{Gr}_u^{1/2}$ and $\mathrm{Gr}_T^{1/2}$). Otherwise, we can proceed as outlined and we again expand ϕ in a Fourier series (essentially setting $\mathrm{Gr}_u^{1/2}\left(\partial_z^{-1} f\right) = -1$ in Eq. (47)) to obtain

$$\frac{\tilde{\mathrm{Ri}}k_x^2}{k_x^2 + k_z^2}\hat{\phi} - k_x k_z\hat{\phi} + \frac{\Gamma}{\mathrm{Re}}\left(k_x^2 + k_y^2\right)^2\hat{\phi} = 0, \tag{48}$$

which allows for nontrivial solutions only if Γ is

$$\Gamma = \frac{\mathrm{Re}k_x k_z}{\left(k_x^2 + k_z^2\right)^2} - \frac{\mathrm{Re}\tilde{\mathrm{Ri}}k_x^2}{\left(k_x^2 + k_z^2\right)^3}. \tag{49}$$

The maximum value of Γ over all wavenumbers k_x and k_z therefore can be calculated by the point in wavenumber space where the gradient of Γ with respect to k_x, k_z is zero (this can be done quickly using polar coordinates). This gives

$$\Gamma_{\max} = \frac{\mathrm{Re}}{4\tilde{\mathrm{Ri}}}. \tag{50}$$

The Richardson number criterion for energy stability is given by $\Gamma_{\max} \leq 1$, i.e.,

$$\tilde{\mathrm{Ri}} \geq \frac{1}{4}\mathrm{Re}. \tag{51}$$

This criterion differs from the one obtained in the previous section in that the power-law dependence on Re is more advantageous. This of course stems from the fact that before we have used relatively crude estimates, whereas here, we calculated the optimal bound.

As we have seen now, in the limit of low Péclet numbers, energy stability can be achieved for large enough $\tilde{\mathrm{Ri}}$, because the temperature perturbation drops out of the equations. It is this slaving of the temperature perturbation to the vertical velocity perturbation that constitutes the main difference between the low Péclet number limit and the general case.

3 Exact upper bounds for body-forced stratified flows

In this section we develop some exact upper bounds for body-forced stratified shear flows in two-dimensional doubly periodic domains. Bounds for energy injection and dissipation in body-forced flows have been investigated in the unstratified case by [5, 1] and for stratified boundary-forced flows by [4, 11]. In [5] the authors derive general bounds on the energy injection in the three-dimensional case, whereas the authors of [1] derive bounds on the energy dissipation in two dimensions using the enstrophy budget. Here, we apply similar mathematical arguments to body-forced stratified flows and show that the arguments used for the unstratified case still hold in the stratified case.

For convenience, the calculations in this section are based on the dimensional momentum equation (1a). The system is assumed to be two dimensional. We start by defining the viscous energy dissipation ϵ and enstrophy dissipation χ as

$$\epsilon = \nu\langle\overline{|\nabla\mathbf{u}|^2}\rangle = \nu\langle\overline{|\omega^2|^2}\rangle, \tag{52a}$$

$$\chi = \nu\langle\overline{|\nabla\omega|^2}\rangle = \nu\langle\overline{|\nabla^2\mathbf{u}|^2}\rangle, \tag{52b}$$

where $\omega = \nabla\times\mathbf{u}$ is the vorticity (a scalar in two dimensions) of the flow field and the overbar denotes a long time average (defined in appendix). Using these two definitions and the Cauchy-Schwarz inequality (see appendix), we can bound the viscous energy dissipation in terms of the root-mean-square velocity U and the enstrophy dissipation

$$\epsilon^2 = \nu^2\langle\overline{|\omega^2|^2}\rangle^2 \leq \nu^2U^2\langle\overline{|\nabla\omega|^2}\rangle = \nu U^2\chi. \tag{53}$$

By bounding the enstrophy dissipation χ, we can therefore simultaneously find a bound for the viscous energy dissipation ϵ. The enstrophy equation can be obtained by taking the curl in two dimensions of Eq. (1a), multiplying by ω and integrating over the entire volume and taking a long time average. This yields

$$\chi = \langle\overline{\psi\omega}\rangle - \alpha g\langle\overline{\omega\partial_x T}\rangle, \tag{54}$$

where $\psi = \nabla\times\mathcal{F}_0 f(kz)\mathbf{e}_x$ is the curl of the forcing. In the calculations that follow, we will also need the total energy and temperature equations, which can be obtained by taking the dot product of the momentum equation with the velocity field and integrating over space and time:

$$-\alpha g\langle\overline{wT}\rangle + \epsilon = \langle\overline{\mathcal{F}_0 f(kz)u}\rangle. \tag{55}$$

Similarly, multiplying Eq. (1b) by T and integrating over the entire volume and time gives the temperature equation

$$\langle\overline{wT}\rangle = -\frac{\kappa_T}{T_{0z}}\langle\overline{|\nabla T|^2}\rangle. \tag{56}$$

The first term in Eq. (54) is treated in [1] and bounded as

$$\langle\overline{\psi\omega}\rangle \leq k_f^2 U\langle\overline{|\mathcal{F}_0 f(kz)|^2}\rangle^{1/2} \tag{57}$$

by integration by parts and Cauchy-Schwarz inequality. Here, $k_f^2 = \langle|\nabla^2 f|^2\rangle^{1/2}/\langle|f|^2\rangle^{1/2}$ is a forcing length scale that is equal to k for Kolmogorov-type forcings. The second term on

the right hand side can be bounded using Young's and the Cauchy-Schwarz inequality (see appendix)

$$|-\alpha g\langle\overline{\omega\partial_x T}\rangle| \le \alpha g\langle\overline{|\omega|^2}\rangle^{1/2}\langle\overline{|\nabla T|^2}\rangle^{1/2} = \frac{\alpha g}{\nu^{1/2}}\epsilon^{1/2}\langle\overline{|\nabla T|^2}\rangle^{1/2}, \tag{58a}$$

$$= \left(\frac{\alpha g T_{0z}}{\nu\kappa_T}\right)^{1/2}\epsilon^{1/2}\left(\frac{\alpha g\kappa_T}{T_{0z}}\langle\overline{|\nabla T|^2}\rangle\right)^{1/2}, \tag{58b}$$

$$\le \frac{1}{2}\left(\frac{\alpha g T_{0z}}{\nu\kappa_T}\right)^{1/2}\left(\epsilon + \frac{\alpha g\kappa_T}{T_{0z}}\langle\overline{|\nabla T|^2}\rangle\right), \tag{58c}$$

$$= \frac{1}{2}\left(\frac{\alpha g T_{0z}}{\nu\kappa_T}\right)^{1/2}\left(\epsilon - \alpha g\langle\overline{wT}\rangle\right) = \frac{1}{2}\left(\frac{\alpha g T_{0z}}{\nu\kappa_T}\right)^{1/2}\left(\langle\overline{u\mathcal{F}_0 f(kz)}\rangle\right), \tag{58d}$$

$$\le \frac{1}{2}\left(\mathrm{RiPeRe}\right)^{1/2} k_f^2 U\langle\overline{|\mathcal{F}_0 f(kz)|^2}\rangle^{1/2}, \tag{58e}$$

where we made use of energy and temperature equations. Here, the three nondimensional numbers are defined in terms of the root-mean-square velocity U

$$\mathrm{Ri} = \frac{\alpha g T_{0z}}{U^2 k_f^2},\ \mathrm{Re} = \frac{U}{\nu k_f} \text{ and } \mathrm{Pe} = \frac{U}{\kappa_T k_f}. \tag{59}$$

We therefore obtain the following bound for the enstrophy dissipation χ:

$$\chi \le k_f^3 U^3 \frac{\langle\overline{|\mathcal{F}_0 f(kz)|^2}\rangle^{1/2}}{k_f U^2}\left(1 + \frac{1}{2}\left(\mathrm{RiPeRe}\right)^{1/2}\right). \tag{60}$$

In order to complete the calculation, we also need to find a bound for $\langle\overline{|\mathcal{F}_0 f(kz)|^2}\rangle^{1/2}/k_f U^2$. This can be done by multiplying the x-momentum equation with $\mathcal{F}_0 f(kz)$ and averaging over the entire volume and time (see [1] for the details) to get

$$\langle\overline{|\mathcal{F}_0 f(kz)|^2}\rangle^{1/2} \le k_f U^2\left(c_1 + \frac{c_2}{\mathrm{Re}}\right), \tag{61}$$

where c_1 and c_2 are constants that depend only on the shape of the forcing function f. Using Eq. (61) we finally obtain

$$\chi \le k_f^3 U^3\left(c_1 + \frac{c_2}{\mathrm{Re}}\right)\left(1 + \frac{1}{2}\left(\mathrm{RiPeRe}\right)^{1/2}\right). \tag{62}$$

This bound for the enstrophy dissipation can be used to bound the energy dissipation. Using Eq. (53), we find a bound for the nondimensional viscous energy dissipation $\epsilon/k_f U^3$ in terms of Ri, Re and Pe

$$\frac{\epsilon}{k_f U^3} \le \frac{1}{\mathrm{Re}^{1/2}}\left(c_1 + \frac{c_2}{\mathrm{Re}}\right)^{1/2}\left(1 + \frac{1}{2}\left(\mathrm{RiPeRe}\right)^{1/2}\right)^{1/2}. \tag{63}$$

This bound illustrates nicely that in two dimensions, the nondimensional viscous energy dissipation approaches 0 asymptotically as $\mathrm{Re}^{-1/4}$. This is different in the unstratified case, where it approaches 0 asymptotically as $\mathrm{Re}^{-1/2}$ (see [1]), but our result reduces to that of [1] when $\mathrm{Ri} = 0$. In both cases however, the viscous energy dissipation approaches 0 as the Reynolds number approaches infinity. This is consistent with turbulence phenomenology where the viscous dissipation is zero for infinite Re in two dimensions.

4 Numerical experiments

In this section, we test some of our theoretical results with direct numerical simulations, and present additional results that relate the heat flux through the fluid to input parameters.

4.1 Model setup

In all that follows, we present two-dimensional simulations in a doubly-periodic box of dimensions $5\pi \times 2\pi$. The resolution varies from 64 to 256 Fourier modes in the vertical and from 364 to 512 modes in the horizontal. The forcing is of Kolmogorov type, with $f(z) = \sin(z)$. In addition, we explore the scaling behavior of vertical heat transport for a variety of $\mathrm{Gr}_u^{1/2}$, $\mathrm{Gr}_T^{1/2}$ and Ri. The code used is pseudo-spectral and uses Fast Fourier Transforms in horizontal and vertical directions.

4.2 Typical results

Typical realizations of the simulations are shown in Figs. 2 and 3 for small and large Ri respectively. We find that, given $\mathrm{Gr}_u^{1/2}$ and $\mathrm{Gr}_T^{1/2}$, for strong stratifications (large Ri), the system systematically displays a bursting behavior, i.e., with periodic relaminarization interrupted by bursts of mixing. For weak stratifications (small Ri) the system displays a quasi-stationary turbulent behavior and the flow field is large scale, with vortices on the same scale as the forcing. We calculate time-averaged quantities by running the simulations for a sufficiently long time and then begin the averaging process after the transient period is over.

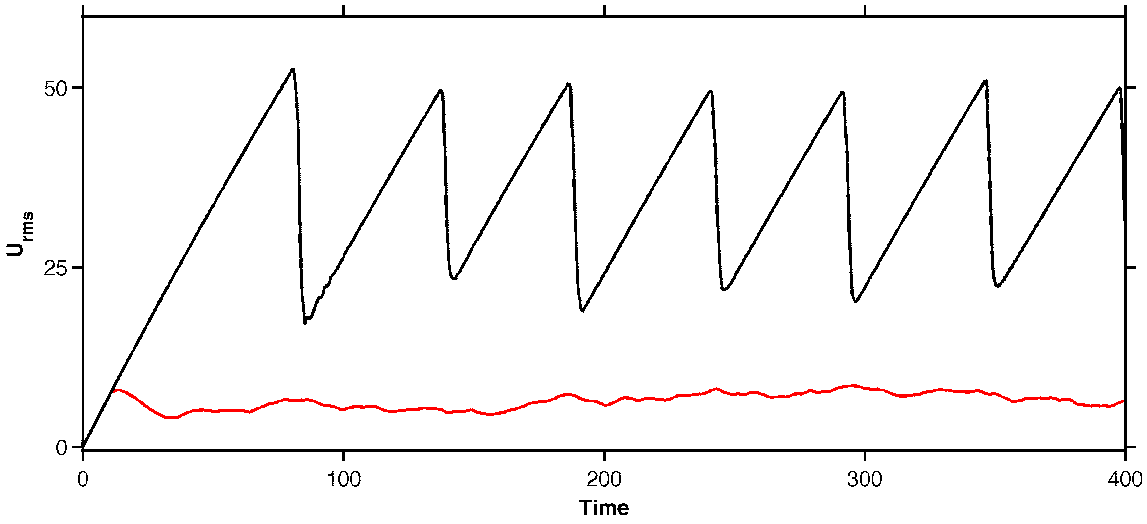

Figure 1: This figure shows two example time series for the large Ri case presented in Fig. 3 (black line) and the low Ri case presented in Fig. 2 (red line). In the case of strong stratification (large Ri) the root-mean-square velocity grows linearly with time until shear instabilities cause mixing. This happens on a quasi-periodic basis. The lower Ri case by contrast, exhibits stationary turbulent flows.

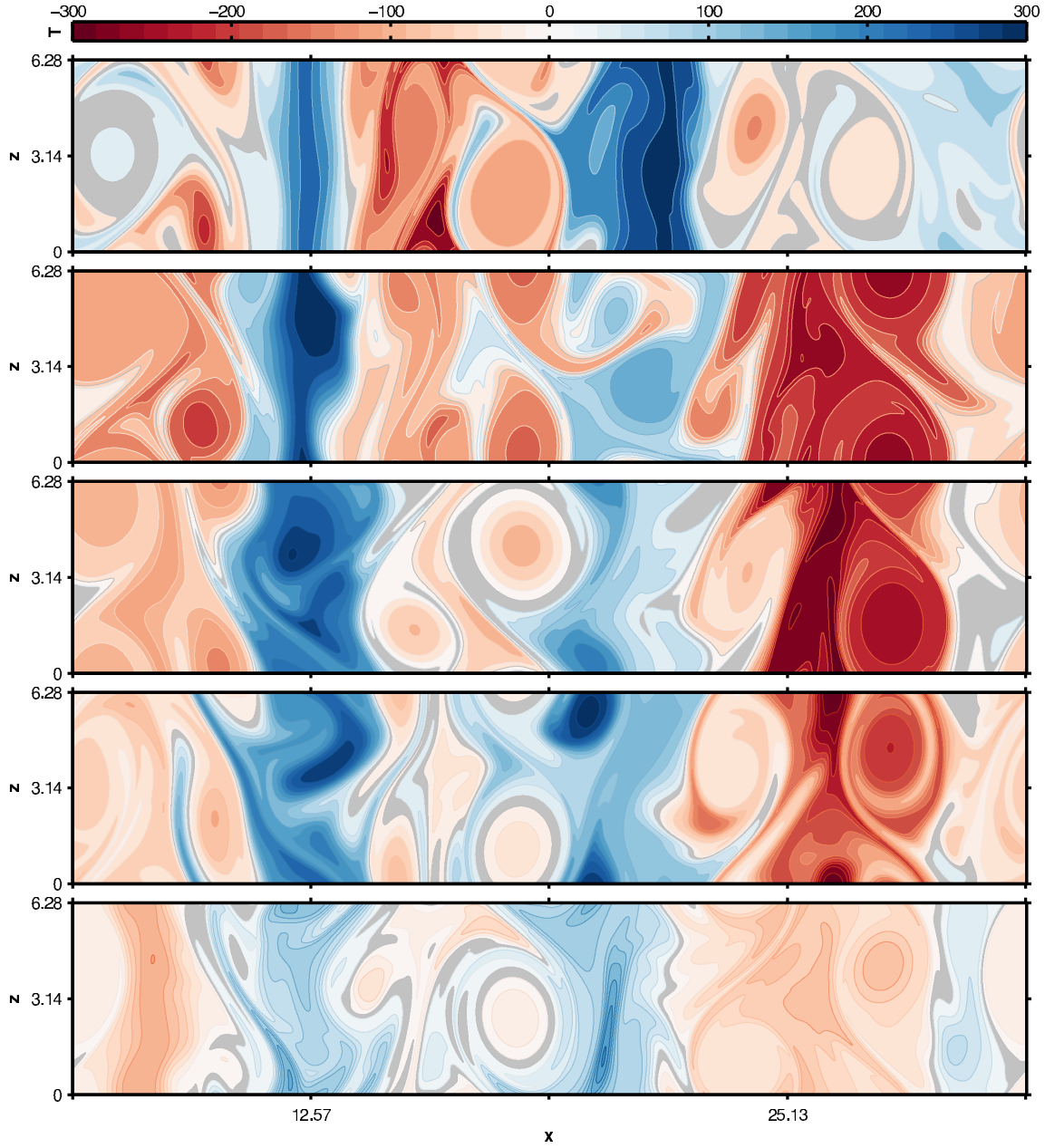

Figure 2: This figure shows a series of typical snapshots of the temperature field for a simulation at $\mathrm{Gr}_T^{1/2} = 100, \mathrm{Ri} = 0.001, \mathrm{Gr}_u^{1/2} = 500$. The flow is dominated by large scale vortices that lead to filamentation of the temperature field and hence to sharp gradients in the temperature field.

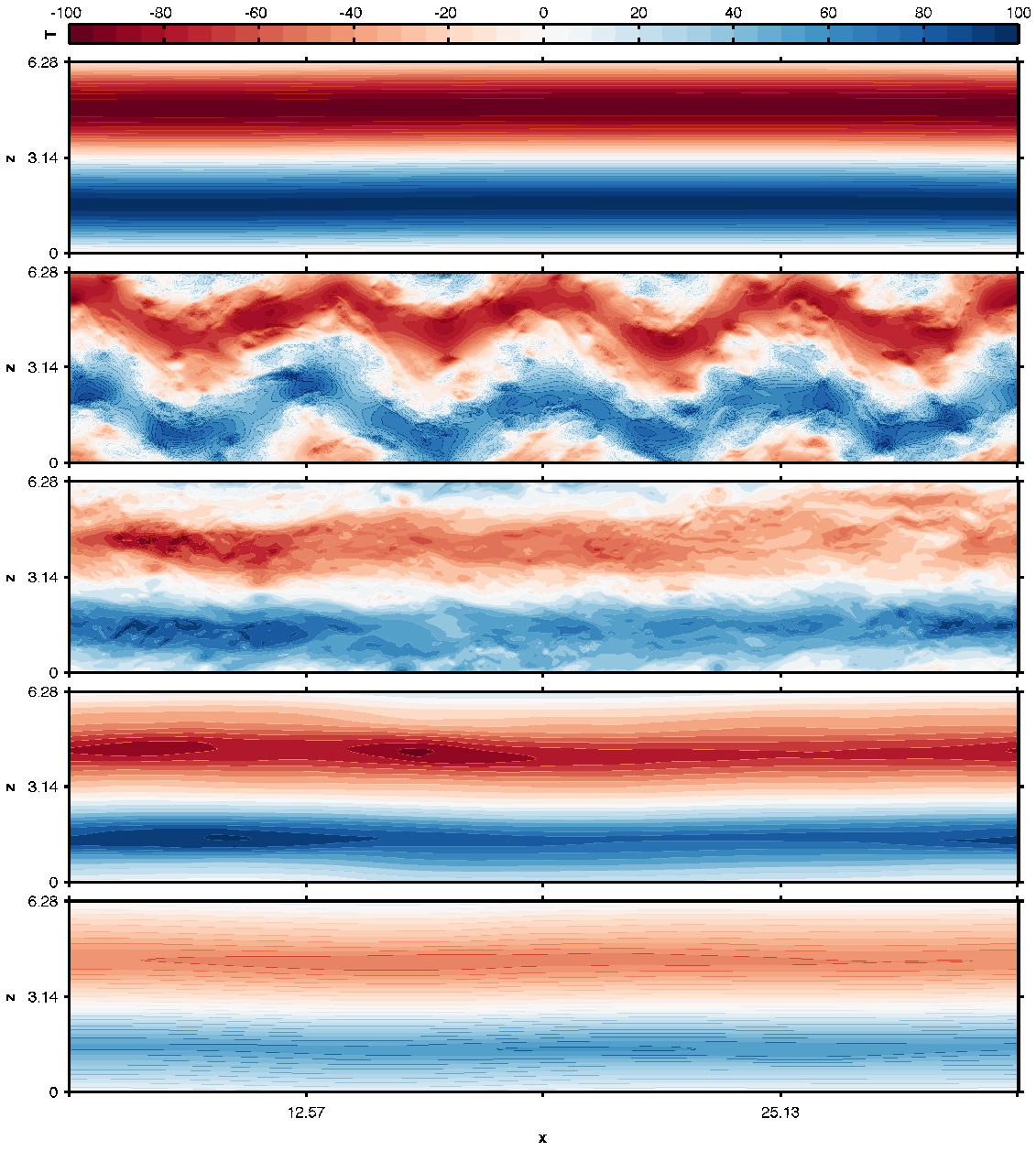

Figure 3: This figure shows a series of snapshots of the horizontal velocity for a bursting simulation at $\mathrm{Gr}_T^{1/2} = 100, \mathrm{Ri} = 1000, \mathrm{Gr}_u^{1/2} = 500$. One can see how the flow goes unstable and then relaminarizes.

4.3 Transport efficiency

An important quantity characterizing a system with stratification is the transport efficiency. It is the ratio of the potential energy used for vertical buoyancy transport to the total energy input into the system, i.e, how much of the injected energy is used for transporting heat compared to being dissipated by viscosity? This efficiency is thus defined as

$$\eta = \frac{-\mathrm{Ri}\langle\overline{wT}\rangle}{\langle\overline{fu}\rangle} = \frac{-\mathrm{Ri}\langle\overline{wT}\rangle}{-\mathrm{Ri}\langle\overline{wT}\rangle + \epsilon}. \tag{64}$$

On phenomenological grounds, one can argue that, at least in two dimensions, the viscous dissipation ϵ tends to zero in the limit of $\mathrm{Gr}_u^{1/2} \to \infty$. This is true if $\mathrm{Gr}_T^{1/2}$ is fixed as $\mathrm{Gr}_u^{1/2}$ increases, because the viscous dissipation approaches zero as long as the root-mean square velocity approaches a constant, while the transport of heat reaches a fixed value. This is equivalent to saying that the transport efficiency η tends to 1 for large $\mathrm{Gr}_u^{1/2}$. We can use the nondimensional temperature equation (essentially Eq. (56)) to replace the vertical transport term in the definition of η and we arrive at

$$\eta = \frac{\frac{\mathrm{Ri}}{\mathrm{Gr}_T^{1/2}}\langle\overline{|\nabla T|^2}\rangle}{\frac{\mathrm{Ri}}{\mathrm{Gr}_T^{1/2}}\langle\overline{|\nabla T|^2}\rangle + \frac{1}{\mathrm{Gr}_u^{1/2}}\langle\overline{|\nabla \mathbf{u}|^2}\rangle}. \tag{65}$$

The phenomenological argument goes as follows: The energy of the velocity field cascades to large scales in two dimensions, which leads to weak gradients. Meanwhile the T field is advected by the velocity field and develops sharp gradients as a result, regardless of Ri. Hence, the transport efficiency therefore approaches 1 in two dimensions. In three dimensions, the situation is generally more complicated, because the viscous dissipation might not approach 0 for large $\mathrm{Gr}_u^{1/2}$. The tracer field might cascade to small scales, but the velocity field is dominated by small scales as well. As $\mathrm{Gr}_u^{1/2}$ approaches infinity (again typically equivalent to the large Reynolds number limit), the viscous dissipation does not approach zero but approaches a finite value. We expect that the transport efficiency will approach a value smaller than 1 which then may depend on the Prandtl number.

We first calculated the transport efficiency for various $\mathrm{Gr}_T^{1/2}$ and Ri, and varying $\mathrm{Gr}_u^{1/2}$, to show that the transport efficiency approaches 1 as $\mathrm{Gr}_u^{1/2}$ increases. We also wish to determine at which point $\eta \approx 1$. Fig. 4 shows the transport efficiency, heat transport and root-mean-square velocity as functions of $\mathrm{Gr}_u^{1/2}$ for different parameter pairs $(\mathrm{Ri}, \mathrm{Gr}_T^{1/2})$ and $(\mathrm{Ri}, \mathrm{Pr})$. We find that the heat transport approaches a constant value as $\mathrm{Gr}_u^{1/2}$ increases, in agreement with a temperature field that is dominated on small scales. As expected, the root-mean-square velocity of the flow does not diverge as $\mathrm{Gr}_u^{1/2}$, but instead also appears to converge to a constant. We find that $\eta \longrightarrow 1$ as predicted, although the rate of convergence seems to depend on the Prandtl and Richardson numbers.

4.4 A scaling for the heat transport based on the Richardson number

In this section, we derive simple scaling laws for the heat flux $\langle\overline{wT}\rangle$ of the flow, based on numerical simulations and heuristic arguments.

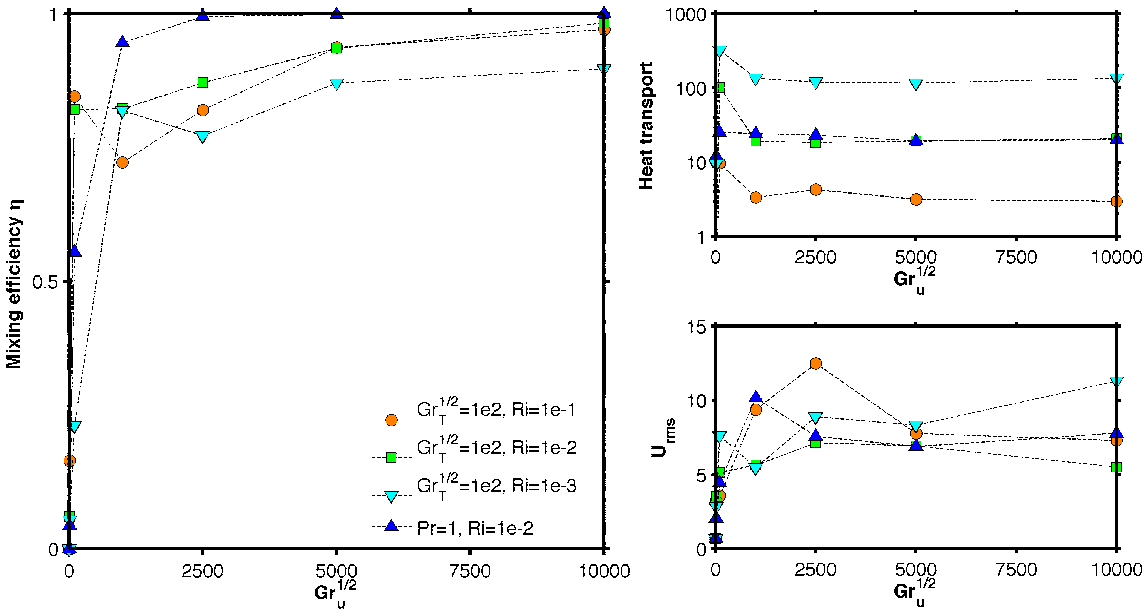

Figure 4: The left panel shows transport efficiency vs $\mathrm{Gr}_u^{1/2}$. Top right panel shows the heat transport vs $\mathrm{Gr}_u^{1/2}$ and the bottom right panel shows the root-mean-square velocity vs $\mathrm{Gr}_u^{1/2}$. As expected, the transport efficiency approaches 1 for large $\mathrm{Gr}_u^{1/2}$ and the root-mean-square velocity remains finite.

4.4.1 The gradient Richardson number

We define a gradient Richardson number in terms of the horizontally-averaged (indicated here as $[(.)]$) temperature and velocity fields as

$$\mathcal{J} = \mathrm{Ri}\frac{1+\partial_z[T]}{(\partial_z[u])^2}. \tag{66}$$

The linear stability of stratified shear flows has been studied at length in [9, 6, 12, 3, 2], and reveals $\mathcal{J}$ to be a critical parameter. At high $\mathrm{Gr}_T^{1/2}$, the flow is linearly unstable, provided $\mathcal{J}$ is less than an $\mathcal{O}(1)$ constant, whose exact value depends on the forcing selected. At low $\mathrm{Gr}_T^{1/2}$, high Ri flows can also be unstable as shown in [7].

4.4.2 Small Richardson numbers, Ri < 1

For low Richardson numbers ($\mathrm{Ri} < 1$), our simulations suggest that $\langle\overline{wT}\rangle \propto 1/\mathrm{Ri}$. We also find that the horizontally-averaged flow projects onto the forcing with

$$\langle\overline{fu}\rangle \sim \mathcal{O}(1). \tag{67}$$

For constant $\mathrm{Gr}_T^{1/2}$, $\mathrm{Gr}_u^{1/2}$, this projection remains of order 1 regardless of the Richardson number as long as $\mathrm{Ri} < 1$. Balancing the heat transport in the energy equation for large

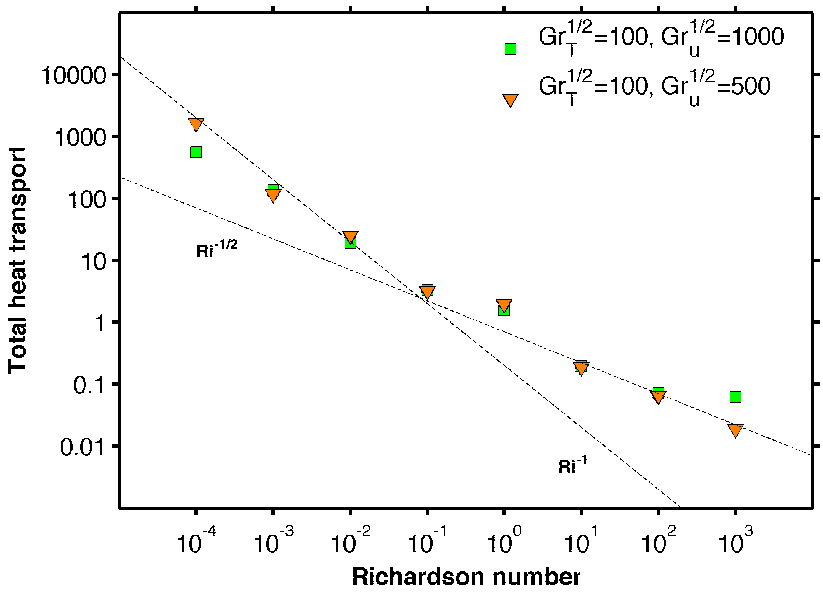

Figure 5: This figure shows the total heat flux through the system $\langle \overline{wT} \rangle$, as a function of the Richardson number. There appear to be two scaling regimes. For low Ri, the flow field is dominated by large vortices that advect the temperature field; we find that $\langle \overline{wT} \rangle \propto \mathrm{Ri}^{-1}$. For high Ri, the system displays a bursting behavior with periods of relaminarization; we find that $\langle \overline{wT} \rangle \propto \mathrm{Ri}^{-1/2}$.

$\mathrm{Gr}_u^{1/2}$ (viscous dissipation approaches 0) then yields

$$\mathrm{Ri}\langle \overline{wT} \rangle \sim \langle \overline{fu} \rangle \sim \mathcal{O}(1) \Leftrightarrow \langle \overline{wT} \rangle \sim \frac{1}{\mathrm{Ri}}, \tag{68}$$

which qualitatively explains the scaling behavior of the heat transport for low Richardson numbers. However, detailed investigations would be necessary to confirm that this scaling holds unambiguously since there is no apriori reason for why $\langle \overline{fu} \rangle \sim \mathcal{O}(1)$ independently of the Richardson number. Furthermore, it will be interesting to determine whether the prefactor depends on other quantities, such as the Prandtl number, for instance in the limit $\mathrm{Gr}_u^{1/2} \longrightarrow \infty$.

4.4.3 Large Richardson numbers, $\mathbf{Gr}_u^{1/2} > \mathbf{Ri} > 1$

At large Richardson numbers, the flow shows a "bursting" behavior (see Fig. 6) which is characterized by times during which the flow field is laminar, with a form $[u](z) \approx a(t)\sin(z)$, where $a(t)$ is a linearly growing function of time. This is halted when the gradient Richardson number drops roughly below 1 (see Fig. 7), at which point the shear goes linearly unstable. The perturbation energy decays again, and the process starts over. This can be used to estimate the heat flux. Indeed, assuming weak temperature gradients as in the laminar solution, we have that a sinusoidal horizontally-averaged horizontal velocity

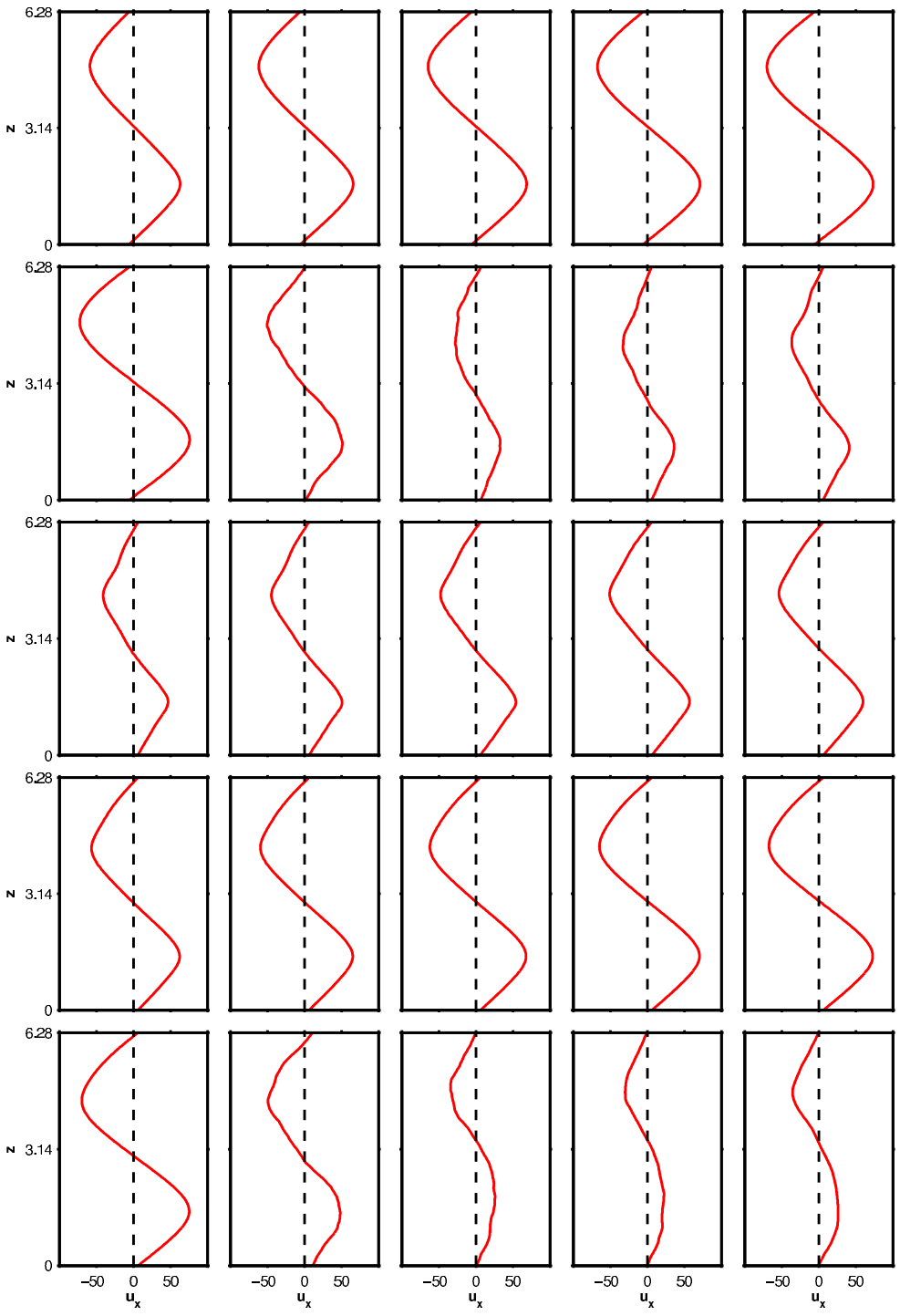

Figure 6: This figure shows, from top left to bottom right, an example of a series of horizontally averaged horizontal velocity profiles from the numerical simulation for $\mathrm{Gr}_T^{1/2} = 100, \mathrm{Ri} = 1000, \mathrm{Gr}_u^{1/2} = 500$. It illustrates that the averaged flow projects strongly onto the laminar solution.

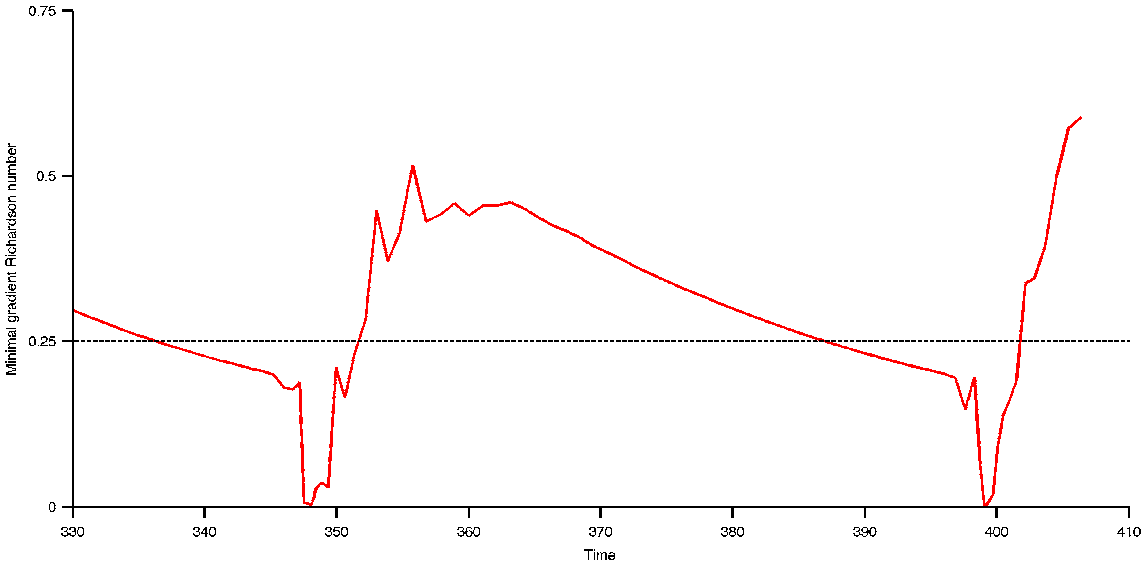

Figure 7: This figure shows a time series for the minimal gradient Richardson number of the flow field for a simulation with $\mathrm{Gr}_T^{1/2} = 100, \mathrm{Ri} = 1000, \mathrm{Gr}_u^{1/2} = 500$. As $\mathcal{J}$ drops below a value of about 0.2 the flow becomes linearly unstable.

profile, $[u] = a(t)\sin(z)$, is linearly unstable if

$$\mathcal{J} \sim \mathcal{O}(1) \Rightarrow \mathcal{O}(1) \sim \frac{\mathrm{Ri}}{a(t)^2 \max_z \{\sin(z)^2\}} \Rightarrow a(t)^2 \propto \mathrm{Ri}. \tag{69}$$

This then implies that $\langle \overline{fu} \rangle \sim \sqrt{\mathrm{Ri}}$. For large values of $\mathrm{Gr}_u^{1/2}$, as previously seen, the viscous dissipation term approaches zero, which then leads to the following balance in the energy equation

$$\mathrm{Ri}\langle \overline{wT} \rangle \sim \langle \overline{fu} \rangle \sim \sqrt{\mathrm{Ri}} \Leftrightarrow \langle \overline{wT} \rangle \sim \frac{1}{\sqrt{\mathrm{Ri}}}. \tag{70}$$

4.4.4 Very large Richardson numbers, $\mathbf{Ri} \gtrsim \mathbf{Gr}_u^{1/2}$

For very large Richardson numbers, the laminar solution is itself linearly stable as shown by [12, 3, 2]. We can estimate the region of the parameter space where the laminar solution is linearly stable using the Miles-Howard criterion for linear stability of stratified shear flows in the inviscid limit [9, 6]. Using our nondimensionalization, we find that the flow is stable provided

$$\mathcal{J} \sim \mathcal{O}(1) \Rightarrow \mathcal{O}(1) \sim \frac{\mathrm{Ri}}{\mathrm{Gr}_u^{1/2}} \Rightarrow \mathrm{Ri} \propto \mathrm{Gr}_u^{1/2}. \tag{71}$$

Because the laminar solution is stable, we have no vertical heat transport as $T = 0$ in this case,

$$\langle \overline{wT} \rangle = 0. \tag{72}$$

Our simulations show that this limit is indeed attained provided $\mathrm{Ri} \gtrsim \mathrm{Gr}_u^{1/2}$.

5 Conclusion and Summary

We have shown that energy stability for stratified shear flows can be achieved for large enough Richardson numbers in the limit of small $\mathrm{Gr}_T^{1/2}$ (similar to a small Péclet number limit). In the general case, the same approach is unsuccessful, in the sense that we find that the energy stability is independent of Ri. In two dimensions, bounds for the viscous dissipation of the system can be extended from the unstratified case to the stratified case. We have shown that standard bounding techniques for forced flows can be applied in much the same way for all values of the Richardson number.

We also argued (at least for the two dimensional case) that the transport efficiency (or mixing efficiency), i.e., the ratio of energy dissipation by vertical transport of heat to the total energy input per unit time approaches 1 in the limit of large $\mathrm{Gr}_u^{1/2}$. This is because energy cascades to large scales in two dimension, whereas the temperature field remains filamented. The dependence of the heat transport on the Richardson number was investigated for constant $\mathrm{Gr}_T^{1/2}$. We found that there are at least three regimes. For $\mathrm{Ri} \gtrsim \mathrm{Gr}_u^{1/2}$ the laminar solution is linearly stable. In the regime of large $\mathrm{Gr}_u^{1/2} > \mathrm{Ri} > 1$, the system displays a bursting behavior. The bursting can be explained by a mean flow profile that strongly projects onto the forcing with an amplitude that periodically grows trying to approach the laminar solution. Because the amplitude of the laminar solution is proportional to $\mathrm{Gr}_u^{1/2}$, it is not linearly stable in this regime, and the system becomes linearly unstable when the amplitude reaches a critical value. In the regime of small Ri the flow is fully chaotic, i.e., the flow field is dominated by large vortices at the forcing length scale that advect the temperature field. The heat transport is no longer achieved by episodic bursts, but is now achieved by the transport induced by these large scale vortices.

6 Acknowledgements

First and foremost, I would like to thank Pascale Garaud and Basile Gallet for their guidance on this project and Charles Doering for helpful discussions on bounding methods and Jacuzzis. I would also like to thank the organizers of this summer school for their efforts in creating an intellectually stimulating environment. However, most importantly, I would like to thank the fellows of the 2013 Woods Hole GFD Summer Program for a wonderful summer, many stimulating discussions and 8 new friendships.

A Averages

We define the volume average in n-dimensions as

$$\langle (.) \rangle = \frac{1}{V} \int (.) \, \mathrm{d}\Omega, \tag{73}$$

where V is the Volume of the domain and $\mathrm{d}\Omega$ is the volume element. We define the long time average $\overline{(.)}$ as

$$\overline{(.)} = \lim_{T \to \infty} \left(\frac{1}{T} \int_0^T (.) \, \mathrm{d}t \right), \tag{74}$$

and the horizontal average $[(.)]$ as

$$[(.)] = \frac{1}{L_x} \int_0^{L_x} (.)\, \mathrm{d}x, \tag{75}$$

where L_x is the horizontal domain size.

B Fourier series

We define the Fourier series of a real-valued zero-mean function $f(\mathbf{x})$ on the periodic domain $[0, L_1] \times \ldots \times [0, L_d]$ as follows:

$$f(\mathbf{x}) = \sum_{\mathbf{k}} \exp\left(i\mathbf{k} \cdot \mathbf{x}\right) \hat{f}_{\mathbf{k}}, \tag{76}$$

for $\mathbf{k} = 2\pi\mathbf{n}$, where $\mathbf{n} = (n_1/L_1, \ldots, n_d/L_d)$ with positive and negative integers n_i. Here, L_i denotes the domain size in the i-th direction and $\hat{f}_{\mathbf{k}}$ is the potentially complex Fourier coefficient associated with the wavenumber vector $\mathbf{k}$. The largest domain size is given by $L_{\max} = \max\left(L_1, \ldots, L_d\right)$ and the total volume is given by $V = L_1 \cdot \ldots \cdot L_d$. We define the norm of the wavenumber vector to be $k = |\mathbf{k}|$ with $k \geq 2\pi/L_{\max}$.

C Basic Inequalitites

C.1 Young's inequality

Young's inequalities can be derived from first principles in the following way:

$$(a+b)^2 = a^2 + 2ab + b^2, \tag{77a}$$

$$(a-b)^2 = a^2 - 2ab + b^2, \tag{77b}$$

$$\Rightarrow -\frac{1}{2}\left(a^2 + b^2\right) \leq ab \leq \frac{1}{2}\left(a^2 + b^2\right). \tag{77c}$$

Therefore, the product $2ab$ can be sandwiched between the sum of the squares. This is useful when it comes to estimating products, since sums greatly simplify the treatment of integrals (compared to products).

C.2 Hoelder's inequality

We prove a simple form of Hoelder's inequality for scalar functions [5]. Given two function f and g, where we only need that g is bounded and f is integrable, we have that at every point

$$f(x)g(x) \leq |f(x)g(x)| \leq \sup_y \left[|g(y)|\right] |f(x)|. \tag{78}$$

Now, we can use this under the integral so that we arrive at the integral inequality

$$\int f(x)g(x)\, \mathrm{d}x \leq \sup_y \left[|g(y)|\right] \int |f(x)|\, \mathrm{d}x. \tag{79}$$

This can be used when information on shape or the boundedness of function is available.

C.3 Poincaré's inequality

Poincaré's inequality can be used to estimate norms of zero-mean functions in terms of the norm of their derivative (or gradient) [5]. We restrict ourselves to finite periodic domains ω of dimension d with largest extent $L_{\max}$. Using Parseval's theorem, we have

$$\int |\nabla f|^2 \,\mathrm{d}\Omega = V \sum_{\mathbf{k}} \mathbf{k}^2 f_k^2 \geq V \sum_{\mathbf{k}} \frac{4\pi^2}{L_{\max}^2} f_k^2 = \frac{4\pi^2}{L_{\max}^2} \int |f|^2 \mathrm{d}\Omega. \tag{80}$$

This allows for useful estimates when dissipation rate terms are involved, i.e., terms of the form $\langle |\nabla u|^2 \rangle$.

C.4 Cauchy-Schwarz inequality

The Cauchy-Schwarz inequality is useful when dealing with product of functions under an integral [5]. If f and g are square integrable scalar functions

$$\left| \int f(x) g(x) \,\mathrm{d}x \right|^2 \leq \int |f|^2 \,\mathrm{d}x \int |g|^2 \,\mathrm{d}x. \tag{81}$$

References

[1] Al Alexakis and C R Doering, *Energy and enstrophy dissipation in steady state 2D turbulence*, Physics Letters A, 359 (2006), pp. 652–657.

[2] NJ Balmforth and Y-N Young, *Stratified Kolmogorov flow. Part 2*, Journal of Fluid Mechanics, 528 (2005), pp. 23–42.

[3] N J Balmforth and Y-N Young, *Stratified Kolmogorov flow*, Journal of Fluid Mechanics, 450 (2002), pp. 131–168.

[4] C P Caulfield and R R Kerswell, *Maximal mixing rate in turbulent stably stratified shear flow*, Physics of Fluids, 13 (2001), pp. 894–900.

[5] C R Doering and C Foias, *Energy dissipation in body-forced turbulence*, Journal of Fluid Mechanics, 467 (2002), pp. 289–306.

[6] L N Howard, *Note on a paper of John W Miles*, Journal of Fluid Mechanics, 10 (1961), pp. 509–512.

[7] F Lignières, *The small-Péclet-number approximation in stellar radiative zones*, Astronomy and Astrophysics, 348 (1999), pp. 933–939.

[8] F Lignières, F Califano, and A Mangeney, *Shear layer instability in a highly diffusive stably stratied atmospheres*, Astronomy and Astrophysics, 349 (1999), pp. 1027–1036.

[9] J W Miles, *On the stability of heterogeneous shear flows*, Journal of Fluid Mechanics, 10 (1961), pp. 496–508.

[10] V Prat and F Lignières, *Turbulent transport in radiative zones of stars*, Astronomy and Astrophysics, 551 (2013), p. L3.

[11] W Tang, C P Caulfield, and R R Kerswell, *A prediction for the optimal stratification for turbulent mixing*, Journal of Fluid Mechanics, 634 (2009), pp. 487–497.

[12] Y-N Young and N J Balmforth, *On stratified Kolmogorov flow*, Stirring and mixing: 1999 Program of Summer Study in Geophysical Fluid Dynamics, (2000), p. 97.